Proc. R. Soc. Lond. A. **329**, 83–103 (1972)
Printed in Great Britain

An atomistic study of cracks in diamond-structure crystals

BY J. E. SINCLAIR† AND B. R. LAWN
School of Physics, University of New South Wales, Kensington, New South Wales, Australia

(*Communicated by F. C. Frank, F.R.S. – Received* 8 *February* 1972)

The structure of atomically sharp equilibrium cracks in diamond, silicon and germanium is calculated. The treatment considers a long plane crack formed by bond rupture across the (111) cleavage plane, critically loaded in tension. Within a small 'core' region immediately surrounding the crack tip the interatomic interactions are represented by a potential function specially constructed to match macroscopic fracture parameters. Anisotropic linear elastic theory is invoked to provide boundary conditions for the core region, and a first approximation for lattice-point displacements within. The core atoms are then relaxed to a configuration of minimum potential energy by computer. The results indicate that continuum theory is capable of giving remarkably accurate predictions of the crack-tip displacement field, except within about three atom spacings from the tip, despite marked nonlinearity in the interatomic force function. These results are discussed in terms of existing continuum models of crack-tip structure: in particular, Barenblatt's model of a cusp-shaped tip region is found to be inapplicable to diamond-structure crystals. The crack-tip geometry is better pictured as a narrow slit terminated by a single line of bonds close to the rupture point. Brief reference is made to the possible extension of the treatment to other classes of highly brittle solid, especially glassy materials, and to the relevance of the results to some fracture problems of practical importance.

1. INTRODUCTION

The fracture of an ideally brittle solid is essentially an atomic process, in which cohesive bonds are ruptured at the tip of the growing crack. Yet traditionally the mathematical treatment of the mechanics of fracture propagation has been developed almost exclusively from continuum concepts. The chief reason for this lies in the interest of simplicity, a proper description of the atomic configuration at a crack tip requiring seemingly formidable analysis in terms of a suitable structural model for the given solid. The continuum approach, based on linear elasticity theory, has in fact proved adequate in many fracture-mechanics problems: in particular, the growth of a semi-brittle crack in most 'engineering materials' can be described in terms of a macroscopic 'plastic zone' encasing the tip.

Many mechanical properties, on the other hand, are highly sensitive to events occurring over distances no greater than a few interatomic spacings. For instance, the energetics of dislocations in plastic crystals, particularly covalently-bonded crystals, may depend largely on the atomic structure of the dislocation core. The ideally brittle crack provides a similar case, the crack front advancing one atomic

† Now at Theoretical Physics Division, A.E.R.E., Harwell, Didcot, Berks., England.

spacing for each line of cohesive bonds ruptured at the tip. The geometrical configuration of bonds immediately surrounding the crack tip may well play a decisive role in a fracture propagation process. In such cases an atomistic description would be warranted.

The question of the fundamental nature of brittle crack propagation is of more than just academic interest. It bears on such practical problems as the influence of a reactive environment on fracture strength, and the path taken by a crack extending through an arbitrary stress field. In each case a proper understanding of the phenomenon demands an interpretation in terms of the bond behaviour at the very tip of the crack itself. Further elaboration on this point will be given in § 4.

In this paper the atomic structure of crack tips in diamond-structure crystals is computed according to a mathematical relaxation procedure. Diamond-type crystals represent possibly the most brittle class of materials at room temperature. Our discussion does, however, extend to other covalent solids, in particular to the widely studied glassy solids. The relaxation method involves the introduction of a suitable interatomic potential function to represent interactions between neighbouring (point) atoms within a prescribed 'core region' surrounding the crack tip. The core boundary is taken sufficiently distant from the crack tip that nonlinear terms in the interatomic force function become tolerably small. Linear elastic continuum theory may then be invoked to supply the boundary conditions for the problem, and to provide a first approximation for the relaxation procedure. Finally, the atomic region is computer relaxed to realise a configuration of minimum potential energy consistent with the conditions at the core boundary.

2. The continuum approach

In this section we outline the continuum approach to the theory of equilibrium cracks. In doing so we shall not make any assumptions about the nature of the tip zone except that new surfaces form there in a thermodynamically reversible manner. We thus invoke the basic notion of Griffith (1920) that for a small extension of an equilibrium crack the increase in free surface energy of the crack walls just balances the reduction in strain energy of the system. Kinetic terms are taken to be zero.

2.1. *Displacement field of a plane crack in an anisotropic linear elastic continuum*

The concept of a crack in a continuum as an internal surface of discontinuity, stress-free over its entire area, forms the basis for present-day fracture mechanics. Starting from this model, several authors have obtained solutions for displacements, strains and stresses around a plane, straight-edged crack in an anisotropic body. For instance, Savin (1961) has solved completely the case of homogeneous two-dimensional loading applied at infinity, while Sih, Paris & Irwin (1965) have given crack-tip solutions for arbitrary loading geometry. Sih *et al.* show that the solutions are very similar to those obtained with isotropic elasticity: in particular,

stress singularities of the order of $r^{-\frac{1}{2}}$ (r being the distance measured from the crack tip) are always obtained.

The crack system considered here consists of a long, plane crack in an infinite body, with one crack edge along the x_3 axis and the other edge parallel to the first and far distant in the negative x_1 direction (figure 1). We shall consider only the

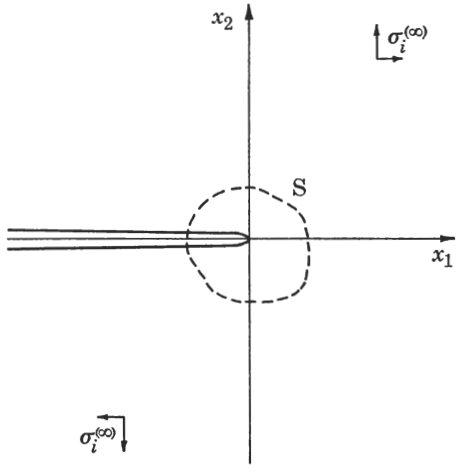

FIGURE 1. The crack system studied. An infinite body contains a plane crack of infinite width in the x_3 direction. The crack lies in the x_1x_3 plane with one edge along the x_3-axis and the other parallel and far distant in the negative x_1-direction. The body is loaded so as to produce a uniform stress $\sigma_i^{(\infty)}$ at infinity.

case where the external loads produce a condition of plane strain perpendicular to the crack edges. Regarding the elastic anisotropy, it is assumed only that there is mirror symmetry about the x_1x_2 plane, for this simplifies the analysis somewhat. The plane strains may then be written in terms of the in-plane stresses as†

$$\epsilon_i = \sum_j a_{ij}\sigma_j \quad (i,j = 1,2 \text{ and } 6). \tag{1}$$

Here the single-subscript notation for stress and strain (defined for instance by Nye 1957) is used.

Sih *et al.* use the standard complex-function method described by Lekhnitskii (1963), whereby the displacements and stresses are expressed in terms of two complex functions $\phi_l(z_l)$, $l = 1,2$, of the variables

$$z_l = x_1 + \mu_l x_2 \quad (l = 1,2). \tag{2}$$

The constants μ_l are obtained from the equation

$$a_{11}\mu^4 - 2a_{16}\mu^3 + (2a_{12} + a_{66})\mu^2 - 2a_{26}\mu + a_{22} = 0, \tag{3}$$

whose roots are μ_1, μ_1^*, μ_2, μ_2^* (two conjugate pairs).

† Note that a_{ij} are modified compliances, since σ_3, linearly dependent on σ_1, σ_2 and σ_6 for plane strain, has been eliminated.

The displacements and stresses are given by †

$$\left.\begin{aligned} u_1 &= \sum_l \mathrm{Re}\,[p_l \phi_l(z_l)], \\ u_2 &= \sum_l \mathrm{Re}\,[q_l \phi_l(z_l)], \\ u_3 &= 0, \end{aligned}\right\} \tag{4}$$

$$\left.\begin{aligned} \sigma_1 &= \sum_l \mathrm{Re}\,[\mu_l^2 \phi_l'(z_l)], \\ \sigma_2 &= \sum_l \mathrm{Re}\,[\phi_l'(z_l)], \\ \sigma_6 &= \sum_l \mathrm{Re}\,[-\mu_l \phi_l'(z_l)], \end{aligned}\right\} \tag{5}$$

where

$$\left.\begin{aligned} p_l &= a_{11}\mu_l^2 + a_{12} - a_{16}\mu_l, \\ q_l &= a_{21}\mu_l + a_{22}/\mu_l - a_{26}, \end{aligned}\right\} \tag{6}$$

and

$$\phi_l'(z_l) \equiv \partial \phi_l(z_l)/\partial z_l. \tag{7}$$

The solution given by Sih *et al.* is

$$\phi_l(z_l) = \frac{\mu_m k_1 + k_2}{\mu_m - \mu_l}(2z_l)^{\frac{1}{2}} \quad (l = 1, 2;\ m = 2, 1, \text{respectively}). \tag{8}$$

Here the real numbers k_1, k_2 are so-called stress intensity factors which are related to the external loading. If the crack length is $2c$ and the loading is uniform stress $\sigma_i^{(\infty)}$ at infinity,‡ we have

$$k_1 = c^{\frac{1}{2}}\sigma_2^{(\infty)}; \quad k_2 = c^{\frac{1}{2}}\sigma_6^{(\infty)}. \tag{9}$$

In this paper we shall consider only tensile loading and take $k_2 = 0$.

It is interesting to note how the solution above is modified by excluding a tip zone, bounded by some cylindrical surface S (figure 1), from the continuum region. Within S, nonlinear behaviour could occur and surface tension forces could become important. With this modification to the original model, the functions $\phi_l(z_l)$ are no longer required to be analytic at the origin, and can be expressed as power series containing positive and negative powers of $z_l^{\frac{1}{2}}$. Assuming finite stresses at infinity, one obtains

$$\phi_l(z_l) = \frac{\mu_m k_1 + k_2}{\mu_m - \mu_l}(2z_l)^{\frac{1}{2}} + \sum_{n=1}^{\infty} (i)^{n-1} \frac{\mu_m \lambda_{1n} + \lambda_{2n}}{\mu_m - \mu_l}(2z_l)^{-\frac{1}{2}n} \quad (l = 1, 2;\ m = 2, 1, \text{respectively}), \tag{10}$$

where the real constants λ_{jn} could be regarded as higher-order stress intensity factors, whose values would depend only on conditions at the inner boundary S. Since the higher-order terms in (10) fall off more rapidly than the principal term

† Expressions (4) and (5) differ from those of Lekhnitskii by a factor of 2, here arbitrarily included in the functions ϕ_l.

‡ The foregoing solution is actually the limit for $c \to \infty$. In this limit, if k_1, k_2 are held constant, then $\sigma_i^{(\infty)} \to 0$, but the profile of the crack-tip remains invariant.

with distance from the tip, they become negligible at distances large compared with the diameter of S (Saint-Venant principle). The simple solution (8) is thus valid at such distances whatever the nature of the tip zone, provided it is small compared with the crack length.

2.2. *Calculations for some specific materials*

The foregoing results give stress and strain distributions for a crack of given length and loading, but do not allow the critical stress intensity factors for crack extension to be determined. This point will be considered in the next section, but it is instructive at this stage to apply the continuum theory to calculate crack-tip geometries for selected brittle solids. We choose to consider fused silica, as representative of the elastically isotropic glassy materials, and silicon, one of the diamond-structure crystals. In both these materials, the covalent bond structure minimizes the possibility of plastic flow under the high crack-tip stress field (Kelly, Tyson & Cottrell 1967).

In the absence of any information regarding surface tension forces or nonlinear behaviour at the tip, let us apply the simple solution† (8) (no doubt beyond its valid range) to determine the displaced contour for $x_2 = \pm \frac{1}{2}r_0$, where r_0 is the interatomic spacing. For this purpose, we shall ignore the 'randomized' structure of glasses and take r_0 as the average silicon–oxygen bond length. The critical stress intensity factors we shall obtain from experimental data.

First, we plot in figure 2 profiles computed using isotropic elasticity with a range of stress intensity factors which may be representative of glassy materials in general. Figure 3 then shows the equilibrium profile for fused silica appropriate to the critical stress intensity factor k_{1c} measured by Wiederhorn‡ (1969) using a double-cantilever fracture technique under carefully controlled conditions (dry nitrogen at 25 °C). Also plotted in figure 3 is the (parabolic) crack contour (broken line) for the ideal continuum surface at $x_2 = 0$.

For the diamond-structure crystals we take the crack plane as (111) and the crack edges perpendicular to the mirror plane $(0\bar{1}1)$. The elastic constants c_{11}, c_{12}, c_{44} referred to the standard cubic axes are transformed for this orientation (see Hirth & Lothe 1968) and the constants a_{ij} then deduced (Sih *et al.* 1965). The constants used for silicon are shown in table 1. Figure 4 shows the equilibrium profile calculated from (4) to (8) and k_{1c} as measured for silicon at liquid nitrogen temperature by Jaccodine (1963).

We note from figures 3 and 4 that the crack tip radii in the continuum limit (the parabolic contours) are small compared with atomic dimensions. For the contours shown $\rho/r_0 \approx 0.9$ (silica), 0.1 (silicon) where the tip radius ρ is given in the isotropic case by $\rho = [2k_1(1-\nu^2)/E]^2$ (Irwin 1958). It is clear from figure 2 that for materials characterized by relatively large stress intensity factors the crack-tip bonds are

† The solutions given for anisotropic elasticity become indeterminate in the special case of isotropy. For this case see, for instance, Irwin (1958).

‡ Our stress intensity factor differs by a factor of $\pi^{\frac{1}{2}}$ from that of Wiederhorn.

likely to stretch well beyond a typical 'linear' range, while for relatively small stress intensity factors the gradual crack-face separation presents a favourable situation for significant cohesive attraction across the interface. These factors require the atomic structure and interactions to be taken into account.

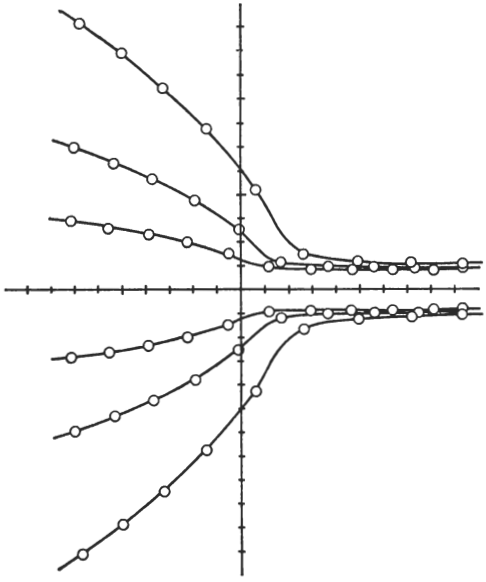

FIGURE 2. Crack profiles for fused silica, computed for $x_2 = \pm \frac{1}{2}r_0$ in continuum-theory displacement field. Curves represent the values 2×10^5, 5×10^5, $10 \times 10^5\,\mathrm{N\,m^{-\frac{3}{2}}}$ for the stress intensity factor k_1. Computed for Young modulus $E = 7.2 \times 10^{10}$ Pa, Poisson ratio $\nu = 0.17$ (Huntington 1958), average Si—O bond-length $r_0 = 0.162$ nm. Circles indicate points originally r_0 apart. The axes are graduated in units 0.1 nm (1 Å).

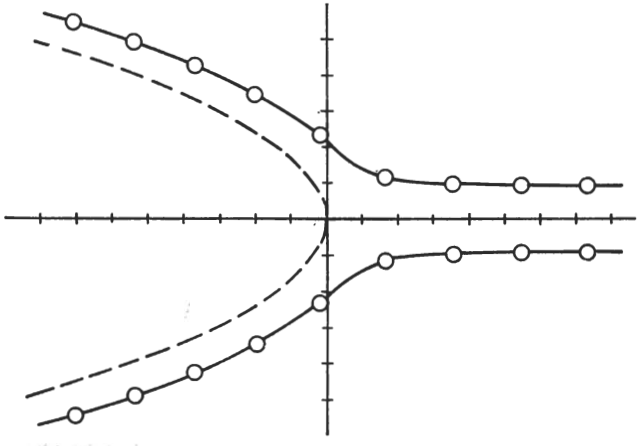

FIGURE 3. Equilibrium profile for fused silica, $x_2 = \pm \frac{1}{2}r_0$ (full line), $x_2 = 0$ (broken line). The critical stress intensity factor is $k_{1c} = 4.5 \times 10^5\,\mathrm{N\,m^{-\frac{3}{2}}}$ (Wiederhorn 1969), E, ν, r_0 as in figure 2. Circles are not to be taken as indicating the solid structure, but only the average atomic spacing.

2.3. *Relation of surface energy and cohesive atomic forces to crack equilibrium*

In his original treatment of the crack problem, Griffith (1920) found the displacement and stress fields about the tip by considering an elliptical cavity in a body under external load. As in the solution given above, the stress became singular at the tip in the limit of zero minor dimension of the ellipse. This physically unrealistic result can be attributed to the atomic dimension of the tip radius, and to the neglect

TABLE 1

		diamond	Si	Ge
experimental data				
nearest-neighbour distance/nm	r_0	0.154 45	0.235 17	0.244 98
elastic constants†/10^{11} Pa	c_{11}	10.76	1.675	1.311
	c_{12}	1.25	0.650	0.492
	c_{44}	5.76	0.801	0.682
sublimation energy‡/10^{-19} J	E_s	11.8	7.46	6.17
calculated quantities				
elastic compliance constants/10^{-13} Pa^{-1}	a_{11}	8.520	53.73	65.55
	a_{12}	−0.408	−11.94	−12.17
	a_{16}	−0.793	−12.00	−16.81
	a_{22}	8.253	50.43	60.71
	a_{26}	0.038	2.67	3.12
	a_{66}	19.646	164.33	199.93
force constants in potential function/N m^{-1}	F_r	472.97	161.55	129.89
	F_ϕ	56.53	9.277	7.722
	$f_{r\phi}$	15.12	3.001	4.050
'range' parameter in potential function/nm^{-1}	α	20.04	14.71	14.51
surface energy/J m^{-2}	γ	5.35	1.46	1.07

† From McSkimmin & Bond (1957), McSkimmin (1953) and McSkimmin & Andreatch (1963).
‡ Converted to J/atom from values in kcal/g atom given by Gschneider (1964).

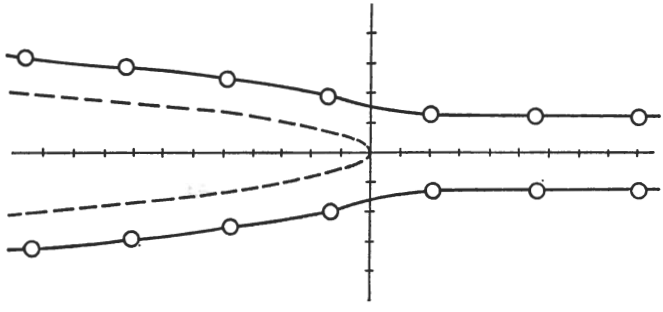

FIGURE 4. Equilibrium profile for silicon crystal, computed from (4), (7) for atom planes at $x_2 = \pm \frac{1}{2}r_0$ (full line), and at $x_2 = 0$ (broken line). Critical stress intensity factor $k_{1c} = 3.76 \times 10^5$ N m$^{-\frac{3}{2}}$ from measurements of Jaccodine (1963); elastic constants and r_0 as in table 1.

of the effect of surface tension forces on the stress distribution. However, despite its neglect in consideration of the stress field, the surface tension was afforded prime importance in Griffith's basic equation

$$G = -\partial U/\partial c = 2\gamma \tag{11}$$

for crack extension equilibrium. Here G is the 'crack extension force' or 'strain energy release rate', arising from reduction in strain energy U per unit crack width upon extension of the crack length c, and γ is the surface energy per unit area. Despite the recognized limitations of Griffith's approach to crack shape, equation (11) stands as the fundamental starting-point for all fracture mechanics.

A significant modification to the description of crack geometry was made by Barenblatt (1962). He proposed that linear continuum theory could validly be employed, even near the crack tip, if it was considered that forces of atomic cohesion, acting across the narrow crack interface, cause the faces to close smoothly in a 'cusp' form. This ensures that the stresses and strains are everywhere finite. A condition for the validity of the model is that the distance, d, from the tip over which cohesive forces are significant should lie in the range $r_0 \ll d \ll c$. That is, nothing in the crack shape or stress distribution should vary appreciably over atomic distances, so that the continuum approach is valid. Theoretical and experimental estimates of d (Cribb & Tomkins 1967; Schmidt & Woltersdorf 1970) have varied from orders of one to tens of atomic spacings, so that the applicability of the model is in some doubt. Nevertheless, regardless of any differences in details of crack-tip geometry, Barenblatt's model is essentially consistent with that of Griffith concerning the condition for equilibrium.

The concept of the existence of a small zone of nonlinearity about the crack tip, as mentioned in § 2.1, has been used in the Irwin–Orowan (Orowan 1949; Irwin 1958) extension of the Griffith equation (11) to the irreversible case of a plastic zone moving with the crack tip. Rice (1968) has shown that specific consideration of the internal structure of the core zone is unnecessary in evaluating the strain energy release rate. He expresses G in terms of a path-independent line integral taken in OX_1X_2 around the crack tip through the surrounding linear elastic region. This integral is also found to be independent of the higher-order terms in (10) (Sinclair 1971*a*), with the consequence that values of G calculated from the simplistic continuum model, in which the higher terms disappear, are perfectly valid. For the anisotropic case with tensile loading ($k_2 = 0$) Sih *et al.* obtain

$$G = \pi k_1^2 a_{22} \operatorname{Im}\left[-\frac{\mu_1 + \mu_2}{\mu_1 \mu_2}\right]. \tag{12}$$

Through (11) this enables the equilibrium stress intensity factor to be related to the surface energy γ. Thus while the status of Griffith's equilibrium equation is preserved, the nature of the crack-tip region becomes a complex nonlinear problem requiring a detailed structural model.

3. The atomistic approach

The major obstacles confronting an atomistic approach to the mechanical behaviour of solids are the lack of fundamental knowledge of interatomic potential functions, and the computational difficulties associated with determining the configuration of minimum free energy for a given structure. The advent of high-speed computers has largely removed the second of these, and atom-relaxation methods have recently been used to describe the core structures of point defects and dislocations in crystals. In many cases, however, sensitivity of the calculation to specific details in the potential functions still proves to be a main limiting factor.

Atom-relaxation methods were first applied to the problem of the mechanical strength of brittle solids by Tyson (1966), who computed theoretical maximum strengths of perfect crystals of several bonding types, subjected to homogeneous shear or tension. Chang (1969, 1970) subsequently simulated a crack in b.c.c. and f.c.c. metals by relaxing to equilibrium atoms in a crystallite containing a narrow (5–20 atom spacings) vacancy sheet. Gehlen & Kanninen (1970) considered a configuration more representative of an ideal cleavage crack, that of two separating adjacent (100) atomic layers in α-iron. One disadvantage of working with materials characterized by metallic bonding is that dislocation nucleation in the crack-tip stress field arises as a possible complication (Kelly *et al.* 1967).

We have used an atomic model to study the configurations of tensile-loaded cracks in the inherently more brittle diamond-structure crystals, diamond, silicon and germanium. Only the atoms near one tip of a long crack are considered explicitly. These atoms form 'region I' ('core'). In 'region II' the remainder of the crystal surrounding region I, the continuum solutions given in § 2 are assumed to apply and are used to calculate the fixed atom positions which supply the boundary conditions for the core region. The atoms in region I are moved to their positions of minimum potential energy as determined from the potential function described in the following subsection.

3.1. *A potential function for diamond-type crystals*

The nature of the bonding in diamond, silicon and germanium is largely covalent. Unfortunately, certain aspects of this bond type are poorly understood at present. In particular, we have little quantitative knowledge of the energetics of large stretching or bending of such bonds, and the nature of possible electron redistribution at free surfaces or internal defects is a subject of some controversy. These factors are relevant to the present problem, in which bonds at the crack tip are strained beyond their limit and new surface area is created. Until our understanding of these difficulties improves, the calculations described below must be considered as first approximations.

Nevertheless, we may hope to demonstrate some of the essential features of the crack-tip structure in brittle solids with the use of a semi-empirical potential, provided it satisfies the following conditions:

(i) The derivatives of the potential evaluated in the perfect-lattice configuration

should be such as to match the observed elastic behaviour, at least for homogeneous strain states, and if possible, also for short wavelength vibrations.

(ii) Under uniform dilation of the perfect crystal the potential energy should be minimum at the true value of the lattice parameter.†

(iii) For large strains the interatomic cohesive forces must be limited, and tend to zero for very large separations.

(iv) The work done in separating atoms across the fracture plane to infinity should yield a reasonable value for the surface energy.

(v) The form of the potential should be such as to account for the brittle nature of the crystal.

Conditions (i) and (ii) can be readily satisfied by the type of potential function assumed in the harmonic lattice dynamics theory, quadratic in the atom displacements from the perfect lattice positions. The other conditions, however, can not. A 'nonlinear' type of potential is required for (iii) and (iv), but potentials such as the Morse function, which produce only central forces, inadequately represent covalent bonds in the solid state. Non-central terms appear to be a prime requirement for (v), and are also necessary for (i) considering the type of anisotropy observed in diamond-type crystals (De Launay 1956).

The potential we propose has the following form. The strain potential energy of a group of atoms displaced from diamond-lattice positions is written as

$$U = \tfrac{1}{2}\sum_i F_r[\Delta_r(r_i)]^2 + \tfrac{1}{2}\sum_{i,j} F_\phi[\Delta_\phi(\phi_{ij})]^2 + \sum_{i,j} f_{r\phi}[\Delta_r(r_i)+\Delta_r(r_j)]\,\Delta_\phi(\phi_{ij}), \tag{13}$$

where

$$\Delta_r(r_i) \equiv (1/\alpha)\,[1-\exp\{-\alpha(r_i-r_0)\}] \tag{14}$$

and

$$\Delta_\phi(\phi_{ij}) \equiv \left(\frac{r_0}{-\sin\phi_0}\right)(\cos\phi_{ij}-\cos\phi_0)\exp\{-\alpha(r_i-r_0)\}\exp\{-\alpha(r_j-r_0)\}. \tag{15}$$

Here r_i is the length of the ith nearest-neighbour bond, ϕ_{ij} is the angle between two bonds $\boldsymbol{r}_i$, $\boldsymbol{r}_j$ from the same atom, r_0 is the perfect-lattice nearest-neighbour distance, and ϕ_0 is the equilibrium inter-bond angle ($\cos\phi_0 = -\frac{1}{3}$ for the diamond lattice). In (13) the sum over i includes all nearest-neighbour bonds, while the double sums over i, j include all distinct pairs of bonds having an atom in common. The constants F_r, F_ϕ, $f_{r\phi}$, α are parameters to be selected.

The construction of this potential function may be explained as follows. For small displacements from the perfect-lattice configuration, (13) is quadratic in the bond-lengths and inter-bond angles. For we have

$$\Delta_r(r_i) \approx \delta r_i \equiv r_i - r_0\text{:}\quad \delta r_i \ll r_0$$

$$\Delta_\phi(\phi_{ij}) \approx r_0\,\delta\phi_{ij} \equiv r_0(\phi_{ij}-\phi_0)\text{:}\quad \delta\phi_{ij} \ll 1;\ r_i, r_j \approx r_0.$$

† Potentials not satisfying this criterion have been used in atomistic calculations, with the holding forces required for stability provided by fixed boundary atoms. However, this would not be possible in the present case where the atomistic region includes part of a free surface, at which no such holding forces could be applied.

Thus for infinitesimal displacements, (13) takes the general form

$$U = \tfrac{1}{2} \sum_n \sum_m H_n F_{nm} H_m, \tag{16}$$

where H_n are displacements (either δr_i or $r_0 \delta \phi_{ij}$) and $F_{nm} = \partial^2 U / \partial H_n \, \partial H_m$ are force constants. Thus we may see that F_r is the force constant for bond stretching, F_ϕ the constant for bond bending, and $f_{r\phi}$ a coupling constant between the size of an angle and the length of its arms.

Equation (16) has the well-known form of a harmonic potential, here in terms not of Cartesian displacements but of internal or 'valence' coordinates – bond lengths, inter-bond angles, etc. Our potential (13) is a nonlinear extrapolation of this quadratic form, selected to give the required behaviour for large strains. In this connection, the parameter α can be selected to give the interactions a 'range'. The behaviour at large strains can be seen from the limits

$$\Delta_r(r_i) \to 1/\alpha \quad \text{as} \quad r_i \to \infty, \tag{17a}$$

$$\Delta_\phi(\phi_{ij}) \to 0 \quad \text{as either} \quad r_i \quad \text{or} \quad r_j \to \infty, \quad \text{independent of } \phi_{ij}. \tag{17b}$$

These ensure negligible force between any widely separated atoms.

The forms of the nonlinear functions Δ_r, Δ_ϕ were selected partly by analogy with the Morse function. We note that the radial terms in (13) may be written

$$\begin{aligned} \tfrac{1}{2} F_r [\Delta_r(r_i)]^2 &= (F_r/2\alpha^2)\,[1 - \exp\{-\alpha(r_i - r_0)\}]^2 \\ &= V(r_i) + D, \end{aligned}$$

where $D = F_r/2\alpha^2$ and

$$V(r_i) \equiv D[\exp\{-2\alpha(r_i - r_0)\} - 2\exp\{-\alpha(r_i - r_0)\}] \tag{18}$$

is the Morse function in r_i. Note that $D = -V(r_0)$ is the binding energy of an atom pair in equilibrium according to this function. Bearing in mind the limit (17*b*) we also see that D is the binding energy per atom pair for the full potential (13). The form of the function Δ_ϕ was selected mainly for computational facility. The change in $\cos \phi_{ij}$ was taken rather than $\delta \phi_{ij}$ because $\cos \phi_{ij}$ is simpler to calculate from the scalar product $\boldsymbol{r}_i \cdot \boldsymbol{r}_j$.

McMurry, Solbrig, Boyter & Noble (1967) have developed a harmonic valence-force potential for diamond, matched to neutron-diffraction dispersion data. Their function employs the valence coordinates δr_i and $r_0 \delta \phi_{ij}$, and assumes six force constants: $F_r, F_\phi, f_{r\phi}$ (as used above), $f_{rr}, f_{\phi\phi}, f_{\phi\phi^*}$. The last three couple adjacent bond lengths, interbond angles sharing a common arm and apex, and interbond angles sharing a common arm but no common apex. The constant $f_{\phi\phi^*}$ brings in fifth-neighbour interactions, while our potential includes only first and second neighbour interactions. These three additional constants could readily be included in our potential, but we have chosen to use only three for the following reasons: (i) the force calculations are greatly simplified by restriction to second-neighbour range;

(ii) exclusion of f_{rr} avoids consideration of atom relaxation at a free surface (see §4.1); (iii) no values for the six constants were available for silicon or germanium; it was considered preferable to select three constants which could be uniquely determined from the three elastic constants c_{11}, c_{12}, c_{44}.

Using the methods described in the appendix, the force constants were determined from the experimental elastic constants, and α from the sublimation energy, for the three materials diamond, silicon and germanium. The results are given in table 1. The sublimation energy rather than the surface energy was chosen for determination of α because of greater accuracy in available data.

3.2. *Relaxation procedure*

The atomic displacements from perfect-lattice positions are calculated from the continuum equations (4), (6) and (8) to provide a first approximation for the adjustable atom positions in region I and the fixed positions in region II. Figure 5 shows

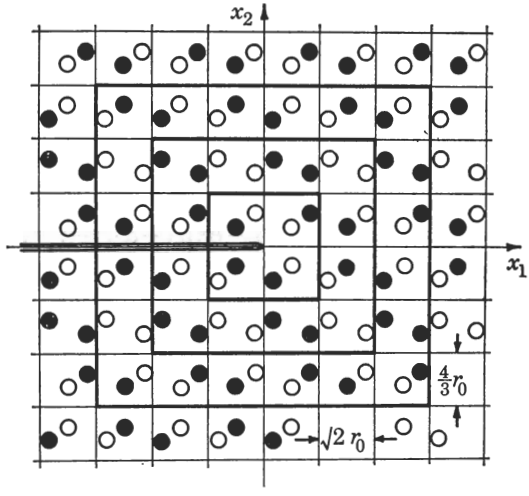

FIGURE 5. Subdivision of diamond lattice into rectangular shells about (111) crack tip for the purpose of labelling atoms in relaxation calculation. Two adjacent $(0\bar{1}1)$ planes are shown (open and closed circles), separated by $\sqrt{2}r_0/\sqrt{3}$ in the x_3-direction. The structure has period $2\sqrt{2}r_0/\sqrt{3}$ in the x_3-direction.

the scheme adopted for labelling individual atoms. The projection of the perfect lattice on the $(0\bar{1}1)$ plane (the x_1x_2 plane) is divided into rectangular cells $\sqrt{(2)}\,r_0 \times \frac{4}{3}r_0$, each cell containing two atoms. The crack tip (origin of x_1x_2) is assumed to lie at the junction of four cells, and region I is then taken as a chosen number of rectangular shells.

The computational procedure adopted to relax region I to equilibrium was the well-known method (Gibson, Goland, Milgram & Vineyard 1960; Gehlen, Rosenfield & Hahn 1968) in which the classical equations of motion of the atoms are integrated, evaluating at each step the total kinetic energy, K. Whenever K reaches a maximum,

the motion is stopped and the integration proceeds from rest. In this way, the potential energy is made to decrease monotonically towards the minimum. The calculation was halted when each resultant force was smaller than a tolerance selected to limit the residual error in nearest-neighbour bond strain to less than 10^{-4}. This condition was reached in typically 100 to 200 time steps.

3.3. *Results*

The core region was cautiously relaxed by progressively increasing the size of region I to include 2, 4, 6 and finally 8 rectangular shells: that is, 512 independent atoms were ultimately relaxed. The resulting atomic configurations are shown in figure 6 for the three diamond-type crystals. Figure 6 shows the progressive stretching of bonds across the crack plane up to and beyond the 'rupture point' as one proceeds in the negative x_1 direction. The exact point of rupture is not simple to specify because of non-central terms in the force function used. However, since the radial force constant F_r is the dominant coefficient in (13), we can, to fair approximation, discuss bond rupture for (111) cleavage solely in terms of the radial (Morse law) component of the force. The bond strain for rupture is then that at which this force component is a maximum. From differentiation of (18) we obtain the critical extension

$$r_c - r_0 = (1/\alpha)\ln 2. \tag{19}$$

Using r_0, α values for silicon (which we discuss here as representative of all three crystals) from table 1, we obtain a rupture strain $(r_c - r_0)/r_0 = 0.20$. From this we assert that all [111] bonds to the left of QT in figure 6*b* have ruptured, while QT and those to the right have not.

The results of more detailed calculations of bond force and strain are shown for silicon in figure 7. One curve indicates the x_2-component of the true bond tension (i.e including bond-bending terms) across the crack plane. (The x_1-components are comparatively negligible.) The concentration of stress at the tip is clearly evident. The length of crack interface across which cohesive forces might be considered significant (Barenblatt's 'd') is no more than three atomic spacings (about 1 nm). The other curve shows the bond strains. The abrupt transition from the 'stretched' to 'ruptured' state of the bonds permits the crack tip to be located to within one atomic spacing. Since in the continuum approximation the crack tip was originally taken to be at the origin in figure 6, we may say that the crack has closed up during relaxation by one atomic spacing.

In order to clarify the changes during relaxation as the size of region I was increased, we have plotted in figure 8 the lengths of the bonds PS, QT, RU (see figure 6*b*) for silicon at each stage. While a trend is discernible to levelling out in values, the ideal of independence of model size has clearly not been reached. One reason for this is that region II is not behaving as a linear continuum, as the model supposes. For from figure 7 it may be seen that even with eight shells in region I, the bond strains at the boundary are approximately 0.02. This lies beyond the

'linear' range for the potential used, the radial force constant, for instance, being 20 % lower at this strain level than that in the unstrained state.

Comparison of figures 6*a*, *b* and *c* reveals no obvious qualitative differences, other than what could be predicted from the continuum theory: the relative magnitude of the surface energy and the elastic constants give diamond a much narrower equilibrium crack profile than the other two crystals. On the atomic level,

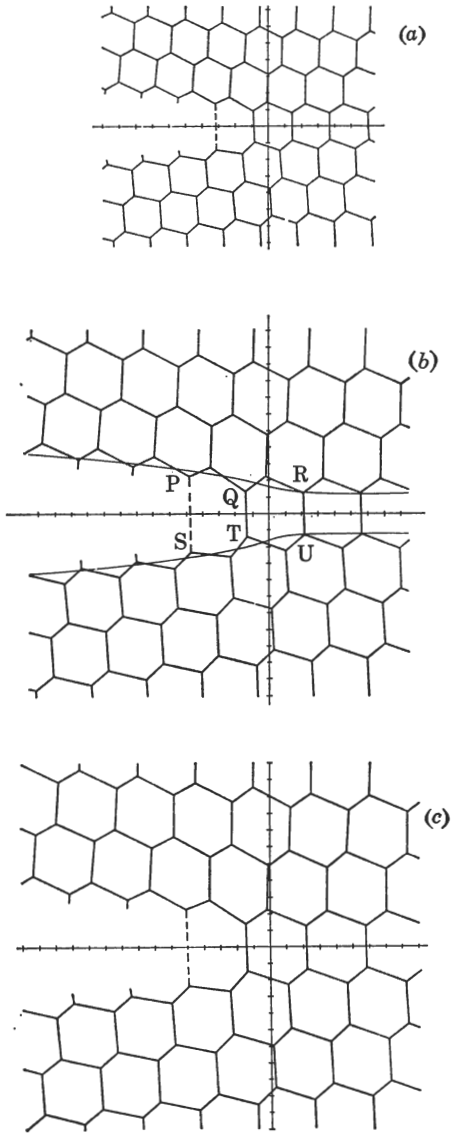

FIGURE 6. Computer-relaxed atomic configuration near equilibrium (111) crack tips in (*a*) diamond, (*b*) silicon, and (*c*) germanium. (0$\bar{1}$1) projection plane (as in figure 5), but only portion of core region is shown. Computed using data in table 1. Axes graduated in units of 0.1 nm (1 Å).

this fact can be understood from the relatively large bond-bending constant, F_ϕ, for diamond which produces a greater resistance to shear deformation around the crack tip than is apparent in silicon or germanium.

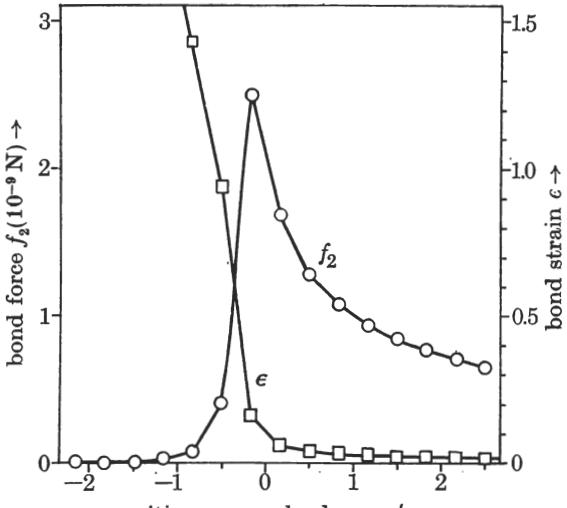

FIGURE 7

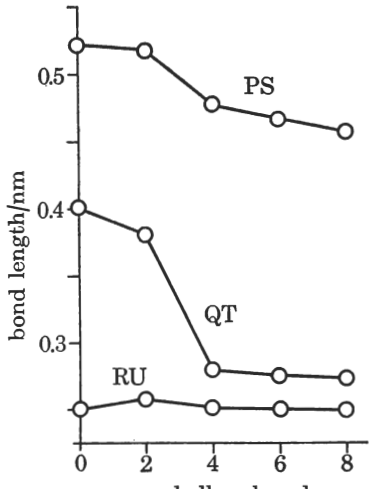

FIGURE 8

FIGURE 7. Plots of strain and tension in the [111] bonds across the (111) crack plane in silicon.

FIGURE 8. Dependence of Si—Si bond-lengths PS, QT, RU (refer to figure 6*b*) on size of relaxed region. As region I is increased from 2 to 4 rectangular shells, the bond QT contracts from the 'ruptured' to the 'stretched' state, thus closing the crack by one atomic spacing.

4. DISCUSSION

4.1. *Reliability of results*

While the size of the relaxed core region influenced strongly the lengths of a few bonds close to the tip, owing to the slight closing up of the crack during relaxation, it had little effect on the surrounding atomic configuration. Let us now investigate the dependence of results on other possible variations in the model.

First, we investigated the effect of modifying the potential for diamond to include the force constant f_{rr} as employed by McMurry *et al.* (1967). This was done by adding the terms

$$\sum_{i,j} f_{rr} \Delta_r(r_i) \Delta_r(r_j) \tag{20}$$

to (13) to give an energy dependence on the relative extensions of bonds having an atom in common. This modification affects the relation of the parameters of the potential to the elastic constants and to the sublimation and surface energies. In particular, if the ith bond is a 'dangling' bond at a free surface ($r_i \to \infty$; $\Delta_r(r_i) \to 1/\alpha$), the terms in (20) lead to a force on coupled bonds $\boldsymbol{r}_j$ lying in the surface. Thus there is now some surface relaxation. However, since this feature of the potential is not based on any physical theory of redistribution of unpaired electrons, to which the true surface structure is no doubt highly sensitive, any conclusions concerning

modifications to the atomic arrangements would have to be viewed with due caution. In fact, in our calculations the effects of this modification were minimal, both in free surface structure and in the arrangement of atoms near the tip. This is not to say, of course, that surface-bond redistribution effects play a minor role in determining atomic structure near a crack tip. But our potential is matched chiefly to bulk properties and is not entirely suitable as a basis for deciding such issues.

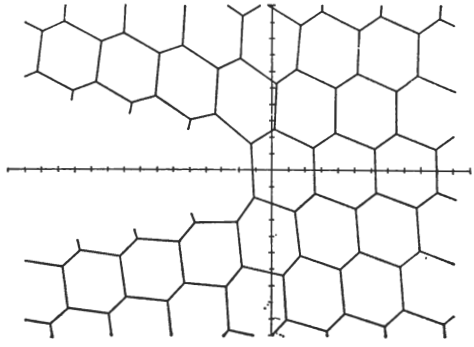

FIGURE 9. Crack-tip structure for germanium (compare figure 6*c*) with modified value of $\alpha = 8.33\,\mathrm{nm}^{-1}$. (Corresponding $k_{1c} = 5.64 \times 10^5\,\mathrm{N\,m}^{-3/2}$.)

The question of bond redistribution is also relevant in matching our parameter α to the sublimation energy. Seeger & Swanson (1968), using a modified Morse potential for defect calculations in silicon and germanium, follow a suggestion of Lidiard (1965) in allowing for the electron promotion energy from s^2p^2 to sp^3 configuration when tetrahedral bonds are formed in a diamond-type crystal. The effect of this consideration is to increase the bond-dissociation energy D (equation (18)) found from a given sublimation energy. We have tested the effect on our calculations of choosing α to agree with the value of D used by Seeger & Swanson for germanium. The implied value of the surface energy is increased, so that the equilibrium crack profile is somewhat wider (i.e. k_{1c} from (11), (12) is larger). The modified result, shown in figure 9, possesses the same qualitative features as found before. The modification to α is probably exaggerated, since we have illogically allowed for bond-redistribution energy on sublimation, but not on surface formation. Moreoever, our original deduced value of k_{1c} agrees more closely with that found experimentally by Jaccodine (1963).

A third point of interest concerns the role of bond-bending terms in the calculation. With only nearest-neighbour stretching terms, the crystal can have no rigidity (De Launay 1956), so that the large angular force constants are certainly required to prevent plasticity effects from occurring. With all our calculations no shear instabilities in the structure were encountered during the relaxation procedure, thus confirming that the diamond structure has sufficient rigidity to sustain a perfectly brittle crack. Of the three crystals, diamond is the most rigid, suggesting that it is least likely to undergo a brittle-to-ductile transition with increasing temperature.

Finally, let us consider the effect of our neglect of the higher-order terms in (10) in fixing the boundary conditions. These terms are possible contributors to the strain field near the tip, and their magnitude would depend on the nature of the atomistic tip zone. The complex matter of finding a self-consistent relaxed atomic configuration and set of higher-order-term coefficients (the λ_{jn} in (10)) has been solved by Sinclair (1971*b*) in a dislocation-core calculation. Sinclair found that the inclusion of such higher terms gave superior 'matching' of the atomistic and continuum regions, and eliminated the dependence of core structure on region I size. We initially attempted in the present calculations to include the higher-order terms in the minimization procedure, but the complexity of the calculations limited the size of region I to five shells. Apparently this was too small for the general continuum solution to apply throughout region II, for convergence in the λ_{jn} values could not be obtained. This was probably due to the nonlinearity of elastic behaviour of the lattice in the large strain field of the crack.

4.2. *Comparison of continuum and atomistic theory*

Except very near to the crack tip, the continuum and atomic-relaxation calculations show close agreement, despite the fact that the elastic non-linearity and the atomicity render continuum theory strictly invalid throughout the core region. This agreement is illustrated in figure 6*b*, in which the continuum solution for the planes $x_2 = \pm \frac{1}{2}r_0$ is superimposed on the atomic configuration. The difference between the two profiles can be chiefly attributed to closure of the crack during relaxation. Even this closure can be explained on a continuum basis, as follows. The strains near the tip are extensional rather than compressive, so that from the curvature of the principal (Morse) term in the force law, we can say that the elastic constants will be effectively reduced in the tip vicinity. This leads us to expect a locally 'blunted' crack profile, which could only be achieved by a shortening of the crack. However, even if we interpret the narrowing of the profile during relaxation to the formation of a Barenblatt-type cusp, we have $d \simeq 3r_0$. Since d is not sufficiently large compared with atomic dimensions we conclude, in agreement with Cribb & Tomkins (1967), that the Barenblatt model is not valid, at least for diamond-structure crystals.

It is of interest to review briefly the possibility of carrying the above arguments over to other classes of brittle material, in particular to the glassy solids of great practical importance. A little consideration shows that comparisons with the above results must be made with due caution. For instance, assuming that the bond-stretching terms in glasses may again be represented by a Morse law for the covalent Si—O bond, we may tentatively anticipate that the predictions of linear continuum theory may once more hold to good approximation except within a few atomic spacings from the crack tip. However, in a glass structure the Si—O bonds will be oriented in somewhat random fashion across the ultimate crack plane so that, unlike the situation depicted in figure 6 where bond rupture may be treated essentially in terms of a stretching mode, other bond deformation modes (e.g. shearing, flexing,

twisting) would require explicit consideration. Further, the possibility that a limited amount of plastic flow may occur at the crack tip cannot be overlooked (Marsh 1964). These factors may explain the linear elasticity prediction of § 2.2, that glasses have a significantly rounder tip profile than the diamond-type crystals. Notwithstanding these differences in behaviour between the two classes of solid, we are led to conclude that the short range of the Si—O bond will be decisive in once more rendering invalid the Barenblatt cusp model. On the other hand, for materials in which the cohesive forces acting across the crack interface are relatively long range in nature, e.g. mica, ionic crystals, etc., we might expect a sufficiently extensive cusp-like region for Barenblatt's theory to be applicable.

4.3. *Implications of the atomistic calculations*

In setting up a brittle-fracture model one often needs to specify conditions at the tip of the crack. But this is the very region where continuum approximations prove to be least representative. The present calculations indicate that for covalently bonded solids the concept of a rounded tip has little physical meaning: rather, the concept of a narrow slit held together at its end by a line of bonds close to the rupture point presents a more accurate picture.

This distinction may, for example, be of importance when considering the practical question of the effect of environmental conditions on brittle fracture. It is well known from studies on glass that cracks propagate more readily in the presence of a reactive gas or liquid, or at elevated temperatures, owing to reduced interatomic cohesion at the crack tip. The mechanism of interaction between environment and cohesive bond is, however, not well understood. Of the theoretical explanations proposed most are sensitive to details in the crack-tip geometry, and most use as their basis the continuum concept of the smoothly rounded tip. The present study suggests that the important region of interaction may be confined to the line of nearly ruptured bonds (e.g. QT, figure 6) across the crack front. Apart from indicating the geometrical aspects of events at the crack tip, the atomistic model also emphasizes that one needs to be careful when specifying the mode of diffusion of a chemical species to the tip bonds. For instance, a molecule which is small enough to diffuse in gaseous form (e.g. O_2 molecule, with O—O separation 0.12 nm) between the crack walls in silicon or germanium, may be forced to undergo surface or even bulk diffusion in the narrower crack region in diamond.

A similar argument may be put forward in discussing the paths of a crack loaded in other than pure tension. Such a problem again requires detailed knowledge of crack-tip geometry (Lawn 1968). It should, in principle, be possible to investigate the effect of a biaxial state of external loading on the crack equilibrium and path in diamond-type solids, but we have not attempted this calculation.

Thus it seems highly probable that many important facets of fracture theory require detailed descriptions of mechanisms on a microscopic scale. Atom-relaxation methods may consequently serve to provide the necessary basis for such descriptions. Consideration of a kinked crack-front structure (Gilman & Tong 1971; Kanninen

& Gehlen 1971) would appear to be the next logical step in the development of a realistic atomistic model.

We are grateful to Professor F. C. Frank, F.R.S., for commenting on the manuscript.

Appendix. Relation of physical properties to the potential

(i) *Sublimation energy*

Consider the perfect crystal to become infinitely dilated. That is, assume all bond-lengths $r_i \to \infty$ while all interbond angles ϕ_{ij} remain constant with value ϕ_0. Then substitution of the limits (17) into (13) yields the energy as $\frac{1}{2}F_r/\alpha^2$ per bond, or F_r/α^2 per atom. Thus the sublimation energy per mole is

$$E_S = N_0 F_r/\alpha^2, \tag{A 1}$$

where N_0 is the Avogadro constant.

(ii) {111} *Surface energy*

Let two-half-spaces of perfect crystal separated by a (111) plane be rigidly separated in the [111] direction. Then only the first term in (13) has a finite limit as the separation tends to infinity, and yields an energy of $\frac{1}{2}F_r/\alpha^2$ per broken bond, or $\frac{1}{4}F_r/\alpha^2$ per surface atom. The limits (17) ensure that all atoms are in equilibrium with no relaxation from the perfect-lattice configuration. Geometrical analysis of the diamond structure shows that there are $\sqrt{(3)}/4r_0^2$ atoms per unit area on the {111} surface, so that the surface energy per unit area for this surface is

$$\gamma = \frac{\sqrt{3}}{16}\frac{F_r}{r_0^2\alpha^2} \tag{A 2}$$

(iii) *Elastic constants*

The derivation of the elastic properties of the diamond lattice from the potential function involves analysis too lengthy to be presented here. As an example of the method, consider the perfect lattice in a state of homogeneous bulk strain so that $\epsilon_1 = \epsilon_2 = \epsilon_3 = \epsilon$; $\epsilon_4 = \epsilon_5 = \epsilon_6 = 0$. Then every bond has length $r_0(1+\epsilon)$ while all interbond angles remain constant at ϕ_0. Then, for small ϵ, we have $\Delta_r(r_i) = r_0\epsilon$, $\Delta_\phi(\phi_{ij}) = 0$ for all i, j, so that the strain energy from (13) is

$$U = F_r(r_0\epsilon)^2 \text{ per atom}, \tag{A 3}$$

and from continuum theory,

$$U = \tfrac{3}{2}(c_{11}+2c_{12})\epsilon^2 \text{ per unit volume}. \tag{A 4}$$

Comparing (A 3), (A 4) we obtain

$$c_{11}+2c_{12} = \frac{\sqrt{(3)}\,F_r}{4r_0}. \tag{A 5}$$

Two other independent relations may be derived by considering other strain states. However, in the general state of uniform strain, the lattice is not homogeneously strained, for each unit cell suffers internal distortion different from that of the lattice as a whole. This fact must be taken into account when deriving atomic displacements from continuum-theory displacement fields.

We find the following three relations between the elastic constants and the atomic force constants:

$$\left.\begin{aligned} c_{11} &= \frac{\sqrt{3}}{12r_0}(F_r + 12F_\phi), \\ c_{12} &= \frac{\sqrt{3}}{12r_0}(F_r - 6F_\phi), \\ c_{44} &= \frac{\sqrt{3}}{12r_0}\left(F_r + 2F_\phi + 4\sqrt{2}f_{r\phi} - \frac{P^2}{Q}\right), \end{aligned}\right\} \tag{A 6}$$

where

$$P = F_r - 4F_\phi - 2\sqrt{2}f_{r\phi},$$
$$Q = F_r + 8F_\phi - 8\sqrt{2}f_{r\phi}.$$

These may be solved to yield F_r, F_ϕ, $f_{r\phi}$ in terms of the c_{ij}.

References

Barenblatt, G. I. 1962 *Adv. appl. Mech.* **7**, 55.

Chang, R. 1969 *Proc. Second Int. Conf. on Fracture, Brighton*, p. 306. London: Chapman and Hall.

Chang, R. 1970 *Int. J. Fracture Mech.* **6**, 111.

Cribb, J. L. & Tomkins, B. 1967 *J. Mech. Phys. Solids* **15**, 135.

De Launay, J. 1956 *Solid St. Phys.* **2**, 220.

Gehlen, P. C. & Kanninen, M. F. 1970 *Inelastic behaviour of solids* (ed. M. F. Kanninen), p. 587. New York: McGraw-Hill.

Gehlen, P. C., Rosenfield, A. R. & Hahn, G. T. 1968 *J. appl. Phys.* **39**, 5246.

Gibson, J. B., Goland, A. N., Milgram, M. & Vineyard, G. H. 1960 *Phys. Rev.* **120**, 1229.

Gilman, J. J. & Tong, H. C. 1971 *J. appl. Phys.* **42**, 3479.

Griffith, A. A. 1920 *Phil. Trans. R. Soc. Lond.* A **221**, 163.

Gschneider, K. A. 1964 *Solid St. Phys.* **16**, 275.

Hirth, J. P. & Lothe, J. 1968 *Theory of dislocations*, chap. 13. New York: McGraw-Hill.

Huntington, H. B. 1958 *Solid St. Phys.* **7**, 213.

Irwin, G. R. 1958 'Fracture', *Handbuch der Physik*, vol. 6. Berlin: Springer-Verlag.

Jaccodine, R. J. 1963 *J. electrochem. Soc.* **110**, 524.

Kanninen, M. F. & Gehlen, P. C. 1971 *Proceedings of Battelle Colloquium on Interatomic Potentials and Simulation of Lattice Defects, Seattle-Harrison* 1971. New York: McGraw-Hill.

Kelly, A., Tyson, W. R. & Cottrell, A. H. 1967 *Phil. Mag.* **15**, 567.

Lawn, B. R. 1968 *J. appl. Phys.* **39**, 4828.

Lekhnitskii, S. G. 1963 *Theory of elasticity of an elastic body*. San Francisco: Holden-Day.

Lidiard, A. B. 1965 *Radiation damage in semiconductors*, p. 336. Paris: Dunod.

McMurry, H. L., Solbrig, A. W., Boyter, J. K. & Noble, C. 1967 *J. phys. Chem. Solids* **28**, 2359.

McSkimmin, H. J. 1953 *J. appl. Phys.* **24**, 988.

McSkimmin, H. J. & Andreatch, P. 1963 *J. appl. Phys.* **34**, 651.

McSkimmin, H. J. & Bond, W. L. 1957 *Phys. Rev.* **105**, 116.

Marsh, D. M. 1964 *Proc. R. Soc. Lond.* A **279**, 420.
Nye, J. F. 1957 *Physical properties of crystals*, chap. 8. Oxford: Clarendon.
Orowan, E. 1949 *Rep. Prog. Phys.* **12**, 48.
Rice, J. R. 1968 *Fracture* (ed. H. Liebowitz), vol. 2, p. 191. New York: Academic Press.
Savin, G. N. 1961 *Stress concentration around holes*. Oxford: Pergamon.
Schmidt, V. & Woltersdorf, J. 1970 *Phys. Stat. Sol.* **41**, 565.
Seeger, A. & Swanson, M. L. 1968 *Lattice defects in semiconductors* (ed. R. R. Hasiguti). University of Tokyo Press.
Sih, G. C., Paris, P. C. & Irwin, G. R. 1965 *Int. J. Fracture Mech.* **1**, 189.
Sinclair, J. E. 1971*a* Ph.D. Thesis, University of New South Wales.
Sinclair, J. E. 1971*b* *J. appl. Phys.* **42**, 5321.
Tyson, W. R. 1966 *Phil. Mag.* **14**, 925.
Wiederhorn, S. M. 1969 *Mechanical and thermal properties of ceramics* (ed. J. B. Wachtman, Jr), Nat. Bur. Stand. Wash. Special Publications no. 303, 217.